Available online at www.sciencedirect.com
ScienceDirect
Cement and Concrete Research 36 (2006) 2086–2097
Cement and Concrete Research

Kneading and extrusion of dense polymer–cement pastes

H. Lombois-Burger [a], P. Colombet [†,a], J.L. Halary [b], H. Van Damme [b,*]

[a] CTG Italcementi Group, rue des Technodes, F-78931 Guerville cedex, France
[b] Ecole Supérieure de Physique et de Chimie Industrielles, PPMD Laboratory, UMR 7615 CNRS-ESPCI-UPMC, 10 rue Vauquelin, 75231 Paris cedex 05, France

Received 27 May 2005; accepted 3 August 2006

Abstract

The kneading and extrusion behavior of dense polymer-containing cement pastes has been investigated. Both the polymer to cement ratio (p/c) and the water to cement ratio (w/c) were varied. Three types of polymers – one adsorbing and two non-adsorbing on cement – were used. The kneading and extrusion parameters (dispersion energy, torque plateau value, extrusion pressure, paste ageing) were determined using instrumented kneader and ram extruder. As will be shown, the most important parameters controlling the efficiency of the kneading and extrusion processes are the cement volume fraction on the one hand and the polymer concentration in the interstitial solution on the other hand. Polymer adsorption is not a key phenomenon, whereas hydrodynamic lubrication is important. A simple free volume model for paste extrusion is proposed.

Keywords: Kneading; Extrusion; Cement paste; Polymer

1. Introduction

In spite of its practical interest, extrusion of cement pastes is a process which has been only moderately investigated and described in the literature [1–5]. Contrary to that of colloidal materials like clays and other fine mineral particles, extrusion of granular materials is intrinsically a difficult process. The size of the particles, large as compared to the range of repulsive surface forces, and the often very irregular particle shape allow for direct frictional particle contacts to occur. Simultaneously, the large size of the voids favours filtration of the liquid through the solid skeleton, thereby increasing the local solid volume fraction. Both friction and filtration may lead to flow blocking through arch formation or jamming. In practice, it has been observed that addition of water-soluble polymers improves dramatically the reliability of the process. When it comes to kneading, which is the compulsory step before extrusion, the available information is even scarcer than for extrusion [6–10].

The present paper is devoted to an investigation of the action of polymers, both on kneading and on extrusion. Both the polymer to cement ratio (p/c) and the water to cement ratio (w/c) were varied. Three types of polymers – one adsorbing and two non-adsorbing on cement – were used. The kneading and extrusion parameters (dispersion energy, torque plateau value, extrusion pressure, paste ageing) were determined using instrumented kneader and ram extruder. As will be shown, the most important parameters controlling the efficiency of the kneading and extrusion processes are the cement volume fraction on the one hand and the polymer concentration in the interstitial solution on the other hand. Polymer adsorption is not an important phenomenon, in contrast to hydrodynamic lubrication.

2. Materials and methods

2.1. Materials

We used an ordinary portland cement (CEM I 42.5) from Italcementi Group, with the following characteristics: Bogue composition, determined from X-ray fluorescence analysis (wt. %): C_3S (56.2%), C_2S (20.2%), C_3A (0.%), C_4AF (16.2%); Blaine surface area: 3680 cm^2/g; average particle diameter: 15 μm; density: 3.2 g/cm^3.

Three polymers were used, with a relatively high molecular mass in order to avoid filtration problems during extrusion: (i) a random acrylic copolymer synthesized by ATO (now Arkema), hereafter referred to as PA, ($M_v = 3.10^5$ g/mol) containing 45 wt. % of methacrylic acid and 55% (w/w) of ethyl acrylate; (ii)

* Corresponding author. Tel.: +33 1 40 79 44 19; fax: +33 1 40 79 46 86.
E-mail address: henri.vandamme@espci.fr (H. Van Damme).

0008-8846/$ - see front matter © 2006 Elsevier Ltd. All rights reserved.
doi:10.1016/j.cemconres.2006.08.001

hydroxypropylmethylcellulose ($M_v \approx 4.10^6$ g/mol), a cellulose derivative named Methocel from Dow Chemicals, hereafter referred to as HPMC; (iii) poly(ethylene oxide) from Aldrich ($M_v = 2.10^6$ g/mol), referred to as PEO. PA was always used in its pre-neutralised form, i.e. with 1 mol of NaOH per mole of methacrylic acid monomer. The most viscous polymer solutions (PEO and HPMC) were homogenised for 24 h before use. As will be shown in Section 3, an important difference between the polymers lies in their ability to adsorb (PA) or not (HMPC, PEO) on the cement particles.

2.2. Adsorption isotherms

In order to quantify the interaction between the polymers and the hydrating cement particles, the adsorption isotherm of each polymer was measured at room temperature. The paste samples were prepared with a constant water to cement weight ratio, $w/c = 0.60$, and variable polymer concentrations in the aqueous phase. After 10 min of mixing, the interstitial solution was extracted by centrifugation and the carbon content determined by total organic carbon analysis (after dilution of the supernatant and removal of dissolved carbon dioxide by flowing N_2 into the solution). The results were corrected for the carbon contained in the water and in the cement particles. The quantity of polymer adsorbed was calculated from the difference between the carbon content in solution before and after mixing with cement.

2.3. Kneading and extrusion

Pastes of given polymer to cement (p/c) and w/c weight ratios were prepared by mixing an aqueous solution of polymer with the cement using a IKA Visc MKD0,6-H60 kneader from IKA. In this apparatus, mixing is ensured by two counter-rotating Duplex bladed paddles connected to the motor through a common shaft and a gearing arrangement which gives a relative velocity reduction of 2:1 at the second kneading arm. The mixing torque is measured at the common shaft by a torsion bar, while an optical revolution counter measures the rotation rate. The temperature of the mixing chamber is regulated at 20 °C thanks to a water bath.

Kneading was operated at 40 rpm (common shaft), in confined conditions (closed mixing chamber, 120 cm^3) in order to optimize the filling of the mixing chamber and to produce a good dispersion thanks to high shear. The volume of cement was always 100 cm^3. Mixing is monitored through the evolution of the torque and is allowed to proceed until a torque plateau is reached. Kneading is then pursued for 3 min under moderate vacuum ($\cong 0.5$ atm) in order to outgas the paste without loosing significant amounts of water by evaporation.

Extrusion was performed using a capillary rheometer (ram extruder equipped with a 10 kN force transducer) having a cylindrical barrel of diameter D equal to 20 or 30 mm, and a 30 or 80 mm long die with a rectangular section of 4 mm × 10 mm. Unless specified, the extrusion was performed with a barrel of diameter 30 mm and a 30 mm long die land. The paste was set up in the barrel, compressed at 14.2 MPa in order to expel the air, and extruded at a constant ram speed adjusted to produce an extrudate velocity of 176.7 mm/min (calculated assuming plug flow in the die land). The pressure gradient between the ram and the atmospheric outlet, more simply named extrusion pressure in the following, was monitored during extrusion. Since, apart from a short initial transient regime, extrusion is basically a constant pressure process all along the ram displacement, we will only consider one single pressure value in each extrusion experiment.

With the strongest pastes, the force range of the 10 kN transducer was not large enough to enable extrusion with the 30 mm barrel, and a barrel of smaller diameter (20 mm) was used. This brings the force within the range of the 10 kN force transducer and, in addition, reduces the contraction through which the paste must flow from the barrel to the die land. In order to convert the extrusion pressures thus obtained into data directly comparable to those recorded with the 30 mm barrel, we used Benbow's model for ram extrusion [11] (the extrusion pressures obtained in this way will be marked with a star on the figures). This model decomposes the extrusion pressure gradient into two contributions: (i) a first contribution due to the plastic deformation of the paste in the contraction from the barrel to the die land and (ii) a second contribution due to the paste flow in the die land, opposing the wall shear stress τ_p supposed to be uniform. The influence of τ_p in the barrel may be neglected due to the surface/volume ratio much smaller in the barrel than in the die land.

In the framework of Benbow's model, the extrusion pressure P writes:

$$P = (\sigma_y + av).\ln\left(\frac{A_o}{A}\right) + (\tau_p + bv).\frac{LC}{A} \quad (1)$$

where σ_y is the bulk plastic yield stress, τ_p is the wall shear stress, A, C and L the cross section, cross perimeter and length of the die land, respectively. A_o is the cross section of the barrel, a and b two constants homogeneous to a viscosity per unit length describing the velocity dependence of the flow, and v the exit velocity of the extrudate (calculated in plug flow conditions). The first term represents the pressure drop in the contraction and the second term is the pressure drop in the die land. Each term has two contributions. The first contribution is related to the bulk yield stress (first term) or to the wall shear stress (second term). Due to slippage at the wall, τ_p is smaller than the true yield stress at the wall. The second contribution (the av and bv terms) represent the viscous contributions related to the fluid velocity. Rather than attempting to determine σ_y and τ_p separately by viscosity measurements, we determined the whole pressure drops, including the velocity-dependent contributions, using extrusion experiments with different die lengths [12].

The volume fraction of mineral in the pastes during kneading was calculated from the mass fractions, using the known density of the cement and the density of the polymer solution. For HPMC and PEO, the density of the solutions was calculated on the basis of a mixing law between water and the polymer. This procedure is not reliable for PA since the electric charges along the skeleton may induce important volume changes upon mixing. Therefore, the solution density was directly measured with an Archimedes' balance using 1-chloro octan as the

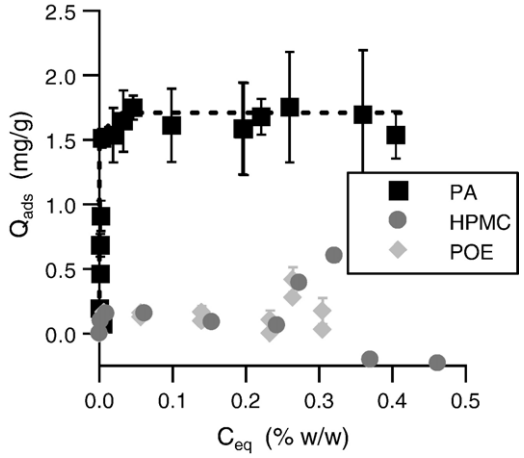

Fig. 1. Mass of polymer adsorbed per unit mass of cement as a function of the concentration (w/w) of polymer in the interstitial fluid at equilibrium.

immersion immiscible solvent. Using these data, a nominal cement volume fraction, ϕ_c, was obtained. For fresh extrudates, ϕ_c was corrected for the quantity of air entrained, estimated from the weight of the fresh samples and the measure of their size some time after extrusion, at the beginning of hardening. This avoids the (difficult) use of a Capellir rule on fresh samples but leads to a small underestimation of the fresh sample section due to shrinkage. Taking the volume of entrained air into account, the real cement volume fraction, ϕ_c^{Re}, was then calculated.

3. Results and discussion

3.1. Adsorption isotherms

The adsorption isotherms obtained by plotting the mass of polymer adsorbed per unit mass of cement vs. the weight concentration of polymer in the interstitial solution at pseudo-equilibrium ("pseudo" because hydration is taking place, though very slowly in polymer-containing solutions) are represented in Fig. 1. For the cement/PEO and cement/HPMC pastes, the carbon concentrations in solution before and after mixing with cement were the same, within experimental error, which means that no adsorption occurs. On the opposite, for the cement/PA pastes, the isotherm is characteristic of a high affinity monolayer adsorption (Fig. 1).

The absence of adsorption of PEO on hydrating cement is in agreement with previous observations [13,14]. The mechanism of EO chains adsorption on mineral surfaces involves either hydrogen bonding with surface OH groups [15,16] or specific bonding to strong Bronsted acid sites [17]. Strong Bronsted acid surface sites are unlikely to exist in the pH conditions of cement pastes and very few OH groups are left on the surface. The overwhelming majority is ionized and those which are left or generated in the hydrates (CSH with high C/S ratio [18], portlandite or the mono-sulfo aluminate phase) are too ionic to make hydrogen bonds [13]. The absence of HPMC adsorption is likely to be due to slightly different reasons. Indeed, previous work has shown that HPMC adsorb on hydrophobic surfaces like talc, but not on hydrophilic surfaces [19]. Considering the very hydrophilic character of cement hydrates, it is unlikely that adsorption through a hydrophobic interaction mechanism might take place.

On the other hand, the negatively charged acrylic copolymer is expected to interact strongly with the positively charged double layer around the cement particles. The zeta potential of C_3S and Portland cement particles in 22 mmol/l $Ca(OH)_2$ solution is slightly positive [20]. Adsorption of negatively charged polymers in these conditions is anticipated and has been demonstrated in the case of carboxylic superplasticizers [21–24].

The purpose of this paper is not to go deeper into the analysis of adsorption. As far as extrusion is concerned, it is enough to conclude that we have two polymers which are present in the interstitial solution only (PEO and HPMC) and one (PA) which is present in the solution and on the solid surface.

3.2. Kneading

3.2.1. Conditions for extrusion: a semi-quantitative analysis

In order to identify the compositions which are suitable for extrusion, it is useful to consider phenomenologically the various cohesion states which are obtained by mixing cement, water and polymer. They are conveniently described in a *p*/*c* vs. *w*/*c* diagram. In practice, a material of given *p*/*c* ratio and *w*/*c*=0.10 was kneaded until the torque reached a plateau value. The physical state of the mixture was then qualitatively characterized using simple criteria such as roughness or smoothness of the external surface, flowability, or the way it may be fractured. The *w*/*c* ratio was then increased and the procedure repeated. As shown in Fig. 2, the diagram obtained presents typically three main zones:

(i) A low cohesion zone at very low *w*/*c*, corresponding either to a humid powder (a powdery solid wet by the dispersing fluid) or to a non-cohesive paste (a single body unable to withstand any mechanical effort other than its own weight).
(ii) A pasty cohesive zone at higher *w*/*c*, subdivided into a hard paste domain at low *w*/*c*, in which the paste undergoes

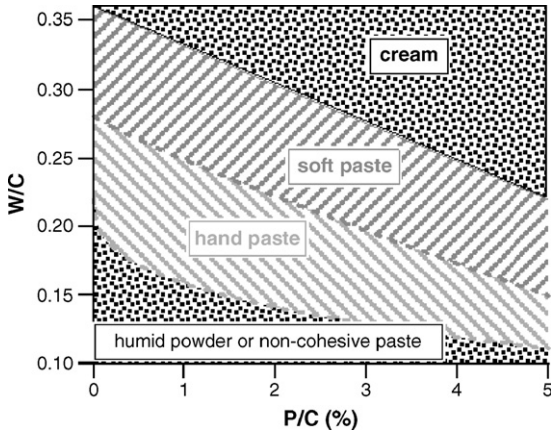

Fig. 2. "Consistency diagram" of PA-containing formulations, describing the consistency obtained after torque's stabilisation for mixtures prepared at given *w*/*c* (*y*-axis) and *p*/*c* (*x*-axis) ratios.

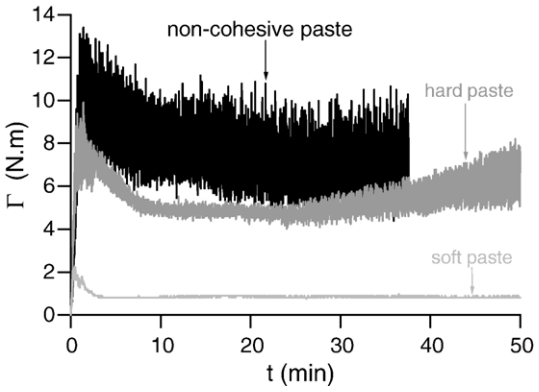

Fig. 3. Typical mixing curves obtained with a non-cohesive paste, a hard paste and a soft paste, respectively. Notice the decrease of noise in this sequence.

brittle fracture under traction or bending, and a soft paste domain at higher *w*/*c*, where the paste undergoes ductile fracture under traction (the fracture regime is easily determined from the complimentarity, or not, of the fracture surfaces). The transition from the non-cohesive zone to the hard paste regime, in addition to the onset of cohesion, corresponds to the *w*/*c* ratio for which the paste starts to reflect light, which is due to the saturation of the void space between particles and to the formation of a liquid film on the surface.

(iii) At still higher *w*/*c*, a cream zone, in which the paste flows on an inclined surface beyond some threshold inclination. The transition from the soft paste to the cream state corresponds to the point where a grove made by a spatula tip is spontaneously healing.

Among the various states just described, only two are suitable for extrusion. Obviously, a humid granular medium cannot be extruded since it is basically a divided solid. A non-cohesive paste is not only non-cohesive and non-saturated (what will be harmful to final mechanical resistance), but it is also a very heterogeneous material as shown by the very noisy character of the mixing curve (torque vs. mixing time) (Fig. 3). A mixture in the cream state is unable to withstand its own weight at die exit. Thus, the two regimes suitable for extrusion are the hard and soft pasty states, for which the noise level of the mixing torque is quite low (Fig. 3), which is the signature of good dispersion state and homogeneity.

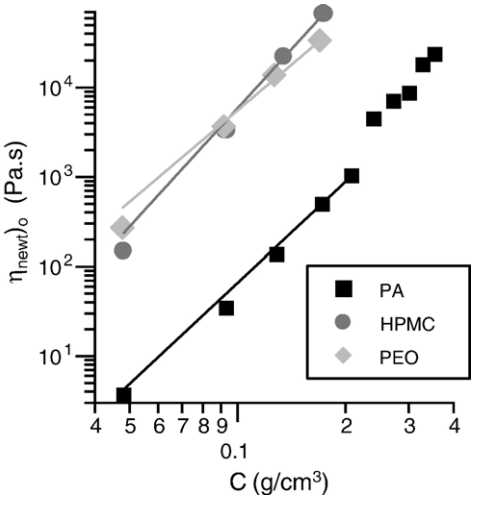

Fig. 4. Concentration dependence of the Newtonian viscosity of the polymer aqueous solutions in ultra pure water (ρ=18.2 MΩ cm).

Two factors – one chemical and one mechanical – may *a priori* influence the quality of dispersion. The first factor is the existence of surface repulsion forces due to adsorbed polymer, thanks to the so-called electrostatic and/or steric mechanisms. This may be the case for PA, but not for HPMC or PEO which do not adsorb. The second factor is the kneading process itself, by breaking aggregates or agglomerates. For two spherical particles of radii r_1 and r_2 in a Newtonian incompressible fluid with viscosity η and in an homogeneous shear rate field, $\dot{\gamma}$ the maximum viscous drag F_{max} is given by:

$$F_{max} = 3\pi\eta\dot{\gamma}r_1r_2 \quad (2)$$

Thus, for a given shear-rate value, the higher the viscosity of the dispersing fluid, the more effective the kneading. In this respect, PEO and HPMC are more effective than PA since, for a given polymer concentration, their solutions are much more viscous, by at least one decade, than PA solutions (Fig. 4).

The quality of dispersion and the respective influence of the two factors just mentioned may be estimated from the volume fraction of cement in a paste at the onset of the hard paste regime, ϕ_c^{hp}. Indeed, assuming that the onset of the hard paste regime corresponds to the solid volume fraction where the paste is a fluid-saturated disordered (or "random"), compact and jammed configuration of particles, the following situations may be considered. If the particles which form the packing are the individual grains of the cement powder (this corresponds to an ideally well dispersed paste), ϕ_c^{hp} would correspond to the theoretical maximum packing fraction calculated from the particle size distribution, ϕ_{max} (for instance, $\phi_{max} \cong 0.65$ for ideally spherical and identical particles). On the other hand, if the paste is less well dispersed and contains aggregates, ϕ_c^{hp} would be lower than ϕ_{max} due to the fluid-saturated voids of the aggregates.

The values of ϕ_c^{hp} for the three polymers and several *p*/*c* ratios are collected in Table 1. It should be noted that the transition from soft to hard paste is sharp enough to determine ϕ_c^{hp} with an accuracy of the order of 0.01. A first observation is that the ϕ_c^{hp} value for plain pastes is much lower than for polymer containing pastes. This may be assigned to flocculation of the cement grains in water and, possibly, to the lower floc-disrupting efficiency of water due to its much lower viscosity (η_o=1 mPa s) as compared to polymer solutions (Fig. 4). A second observation is that the highest (and constant) ϕ_c^{hp} values

Table 1
Cement volume fraction characteristic of the onset of the hard paste state

P/*C* (%)	0	2	3	4	5
PA	0.59	0.67	0.67	0.67	0.67
HPMC		0.67	0.67	0.65	0.64
PEO		0.63	0.63	0.64	0.64

The accuracy is of the order of 0.01.

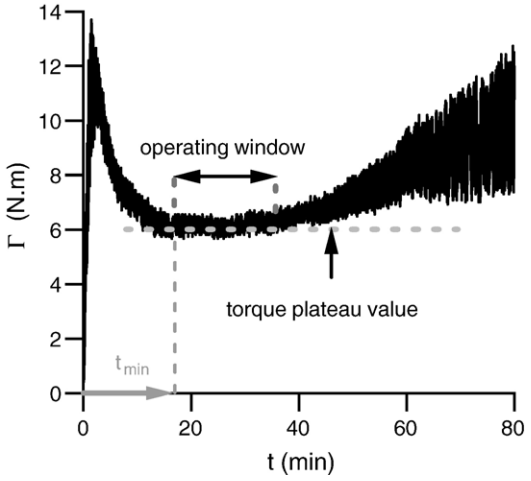

Fig. 5. Typical mixing curve obtained with a hard paste (in this case, a PA containing paste, prepared at $w/c=0.14$ and $p/c=3\%$).

are obtained with PA, showing that this polymer is particularly effective for deflocculation. The relatively lower dispersing efficiency (lower ϕ_c^{hp}), on the average, of HPMC and PEO with respect to PA, in spite of their higher viscosity, suggests that the shear-induced stresses are less effective for deflocculation than the repulsive surface forces. However, the good deflocculation obtained with HPMC at low polymer concentration (2 and 3%) suggests that things are not as simple as that, and that another parameter may be responsible for the (apparently) lower dispersing efficiency of HMPC at high concentrations and PEO at all concentrations. A possible factor which may interfere is the poor solubility of HPMC and PEO, due to their very high viscosity, precisely.

3.2.2. Shape of the kneading curve

From now on, only hard or soft pastes will be considered. A typical mixing curve (torque Γ vs. mixing time t) is shown in Fig. 5. Four regimes may be identified:

(i) A quasi-linear rising regime, from zero torque at the start of kneading, when there are two separated constituents – the cement powder and the aqueous polymer solution – to a torque peak, when one single macroscopically uniform mass is obtained. This is the so-called distributive mixing phase [25], at the end of which all the particles are incorporated in the dispersing fluid but the dispersion is still heterogeneous at microscopic level.

(ii) A decreasing torque regime from the peak down to a plateau value. This is the so-called dispersive mixing phase [25], in which the local particles volume fraction is homogeneized. The decrease of torque may primarily be assigned to the fact that, as dispersion proceeds and aggregates are destroyed, the effective solid volume fraction decreases. In parallel, it seems reasonable to assume that, as the newly created individual particles or floc fragments separate from each other, the hydrodynamic dissipation decreases. Indeed, in concentrated suspensions, the main source of energy dissipation is squeeze flow in the contact regions [26].

(iii) A torque plateau regime, assigned to optimal dispersion in the operating conditions. The length (in time) of this plateau is the operating window for extrusion.

(iv) Last, a torque re-increase regime which, as will be shown later, may be assigned to accelerated setting.

The torque peak value is roughly related to the viscosity of the dispersing fluid and to the mineral loading, but it is very dependent on the way the constituents are loaded into the mixing chamber. Hence it is very variable from one experiment to another and it will not be discussed further. In the following, we will concentrate our analysis on the energy required to reach optimal dispersion (i.e. the torque plateau at $t=t_{min}$, Fig. 5), on the torque plateau value itself, Γ_p, and on the anticipated setting.

3.2.3. Torque plateau value Γ_p

When the torque plateau is reached, the paste may be considered as a macroscopically and microscopically homogeneous medium. Γ_p may be normalized with respect to the total volume of the medium which is sheared, and which is the paste volume,

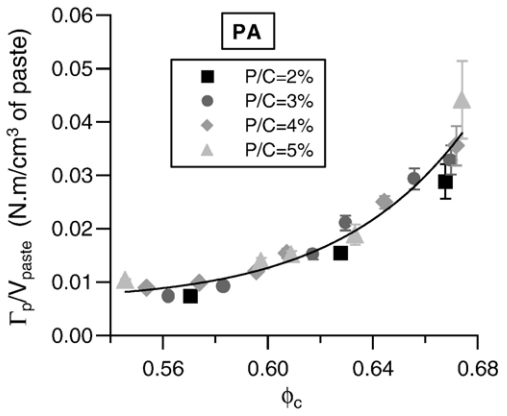

Fig. 6. Torque plateau value per unit volume of paste vs. cement volume fraction for PA containing pastes.

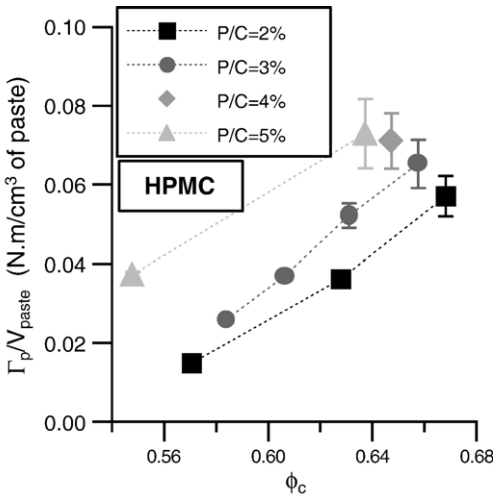

Fig. 7. Torque plateau value per unit volume of paste vs. cement volume fraction for HPMC containing pastes.

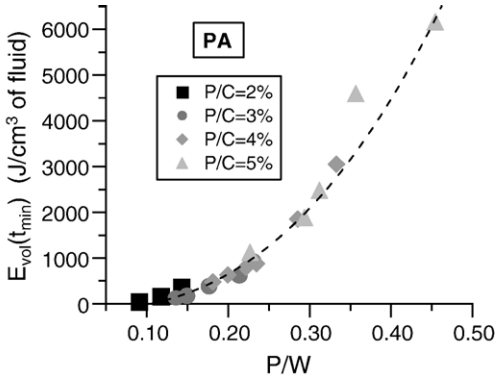

Fig. 8. Dispersion energy per unit volume of interstitial fluid vs. polymer to water ratio (p/w) for PA containing pastes.

V_{paste}. This torque plateau value per unit paste volume, Γ_p/V_{paste}, is plotted vs. cement volume fraction in Figs. 6 and 7 for PA and for HPMC, respectively. For both polymers, at constant p/c, Γ_p/V_{paste} is found to increase with ϕ_c: the higher the mineral loading of the paste, the higher the normalized torque plateau value. On the other hand, at constant ϕ_c, the variation with p/c depends on the polymer considered. For PA pastes, in which the interstitial fluid is the less viscous, Γ_p/V_{paste} is independent of p/c. Thus, a master curve is obtained, fitting all the data points for PA (Fig. 6). On the contrary, for HPMC pastes, in which the interstitial fluid is the more viscous, Γ_p/V_{paste} increases with P/C. Hence, the normalized torque plateau value depends on both mineral loading and interstitial fluid viscosity (Fig. 7).

3.2.4. Dispersion energy

The mechanical energy E used for kneading can be calculated from the mechanical power P:

$$P = \frac{dE}{dt} = N.\Gamma \tag{3}$$

where N is the angular velocity of the common shaft and Γ the torque. Hence, if Ω is the rotating speed (rpm) of the common shaft, the mechanical energy is:

$$E(t) = 2\pi\Omega.\int_0^t \Gamma.dt \tag{4}$$

The mechanical energy required to reach an optimal dispersion is $E(t_{min})$, where t_{min} is the time for which the torque plateau value is reached. $E(t_{min})$ contains several contributions, among which is the energy required to disperse the fluid through the granular skeleton. This contribution should depend on the fluid volume. In order to compare data which are free from this fluid volume effect, we normalized $E(t_{min})$ by the volume of dispersing fluid. We thus obtain a quantity that we call a *dispersion energy per unit volume of interstitial fluid*, E_d^{vol}.

Fig. 8 displays E_d^{vol} vs. p/w for PA containing pastes. The polymer concentration regime in which these measurements were performed was always far above the concentration required to reach the plateau of the adsorption isotherm (Fig. 1). One single master curve is obtained for all the data points relative to varying P/C ratios. This suggests that, for a given polymer, and as long as the amount of polymer on the surface is constant, E_d^{vol} depends only on the interstitial fluid's viscosity, which is an increasing function of p/w.

In order to check this assumption directly, not only for PA but also for HPMC, E_d^{vol} was plotted vs. the Newtonian viscosity η_o of the polymer aqueous solution in ultra-pure water (ρ=18.2 MΩ cm) at the same polymer concentration as the interstitial solution (Fig. 9). For a given polymer, the data relative to varying p/c ratios fall again on a master curve. However, the relationship is not linear. The correlation may be fitted with a power law, $E_d^{vol} \sim \eta_o^{\alpha}$ with α=0.69 and α=0.18 for PA and HPMC, respectively. This suggests that non-linear effects are coming into play, such as the influence of the high cement solution ionic strength or local shear rates in the kneader beyond the Newtonian regime.

3.2.5. Torque re-increase and accelerated setting

The final regime on the kneading curves is a regime in which the torque is re-increasing, as illustrated in Fig. 5 for a PA-based paste. Interestingly, this re-increase is also observed with plain (i.e. polymer-free) pastes, with a comparable magnitude (Fig. 10). This rules out any explanation in terms of cement–polymer interactions, or in terms of polymer network formation as suggested for MDF cements [27,28]. Actually, the water–cement interaction and the surface refreshment action of the kneader seem to be responsible for the observed behavior. Indeed, if, in plain pastes, water is replaced by an equal amount of an organic non-reactive solvent like 2-methyl propan-1-ol for instance, the torque remains at its plateau value, with no sign of re-increase (Fig. 10). This suggests that a hydration and setting phenomenon is occurring. This is confirmed by the very intense heat production during torque re-increase, which prevents the thermostating bath from maintaining the kneader chamber at constant temperature.

Another confirmation comes from an experiment in which a PA containing paste of W/C=0.14 and P/C=2% is over-kneaded for a time Δt_{ok} beyond the time required to reach the torque plateau value (t_{min}). As shown in Fig. 11, the resulting

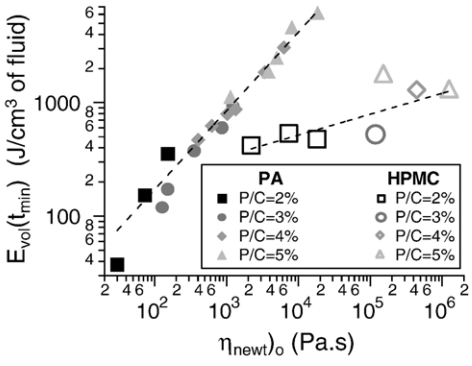

Fig. 9. Dispersion energy per unit volume of interstitial fluid vs. the Newtonian viscosity of the polymer solution in ultra-pure water (ρ=18.2 MΩ cm) at the same polymer concentration as in the interstitial solution.

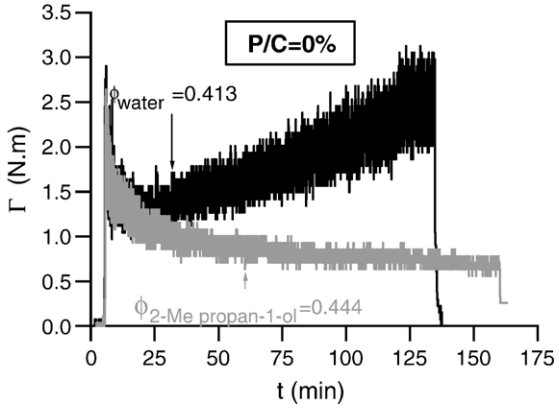

Fig. 10. Mixing curves (torque vs. time) obtained with plain pastes in water or in 2-Me propan-1-ol.

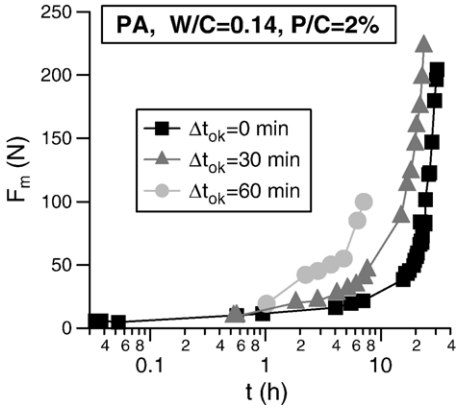

Fig. 11. Texturometer curves obtained with PA containing pastes prepared at $w/c=0.14$ and $p/c=2\%$, over-kneaded for different Δt_{ok} times.

setting time measured with a texturometer and calculated by using t_{min} as time origin is significantly advanced, and all the more as Δt_{ok} is longer.

This confirms the idea of an accelerated setting due to continuous kneading of the components. In order to decide whether attrition of cement grains is responsible for this or not, a plain cement paste was kneaded in 2-methyl propan-1-ol for time periods ranging from 15 to 90 min. The particle size distribution was measured and compared to the initial distribution. No significant difference was observed, which shows that the production of fine or ultrafine particles by attrition is not the reason for accelerated setting. The alternative left is that the intergranular friction during kneading is continuously refreshing the nuclei-covered solid/solution interface, thereby increasing dramatically the number of nuclei. This is in agreement with recent studies on nucleation and growth on CSH/C_3S surfaces [29].

This discussion raises the question of the very nature of the kneading plateau. The previous considerations suggest that it could correspond to a stationary state in which the rate at which hydration stiffens the structure is compensated by the rate at which the aggregated structure continues to be broken down. However, this is not consistent with the existence of an indefinitely long plateau when cement is kneaded in alcohol, i.e. in a medium where no hydration occurs. A more satisfactory hypothesis would be that, like in all concentrated dispersions, the torque plateau value corresponds simply to the stationary state viscosity of a medium in which attractive surface forces (van der Waals forces or ionic correlation forces for instance) are in competition with hydrodynamic forces. In this respect, the shorter time to reach the plateau in the plain (polymer-free) cement pastes in water could be due to the contribution of the attractive forces between the nascent hydrates.

3.3. Extrusion

3.3.1. Ageing

It was observed that the extrusion pressure of a given paste increases with resting time after kneading. To quantify this trend, extrusions were performed with different samples taken from the same paste batch after increasing ageing times. The ageing (or resting) time Δt is taken equal to the difference between the end of kneading and the start of extrusion. In addition, after a given ageing time, several paste samples were re-kneaded and then let ageing again. In that case, the ageing time is defined as the time between the end of the last kneading and extrusion. No compression of the paste was done in these experiments, in order not to shear the paste after kneading and not to perturb the ageing process.

As illustrated in Fig. 12, the extrusion pressure is increasing with Δt. In addition, for a given composition, all the data points fall on one single curve, whether the paste was re-kneaded or not. This shows that, as long as the ageing time is shorter than the setting time, re-kneading is able to rejuvenate the paste in a state indistinguishable from its state after the first kneading. This reversibility rules out that ageing is due to water evaporation.

Physical ageing phenomena have been extensively studied in polymers and are now also well documented in a variety of soft condensed matter systems, including concentrated colloidal suspensions of silica or clay particles for instance [30,31]. There, they were interpreted in terms of slow collective rearrangements

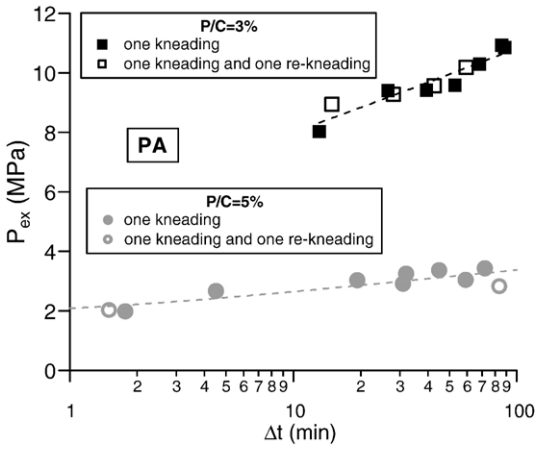

Fig. 12. Extrusion pressure of PA containing pastes prepared at $w/c=0.14$ vs. ageing time Δt (time separating the end of kneading from extrusion) for pastes kneaded once or twice.

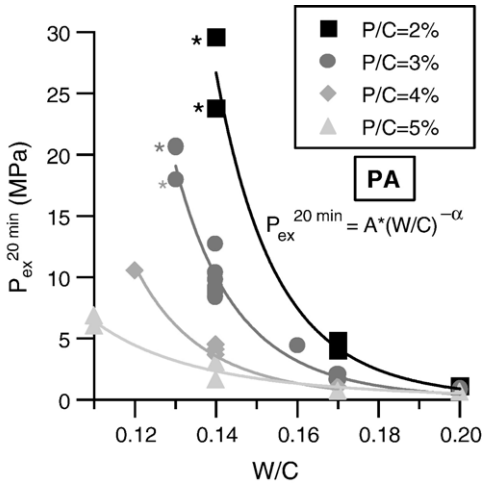

Fig. 13. Extrusion pressures interpolated at an ageing time of 20 min vs. *w/c* ratio for PA containing pastes. The stars indicate the extrusion pressures obtained with a barrel of 20 mm of diameter converted to values expected with a 30 mm diameter barrel, using Benbow's model.

in a many particles system exploring its configurational space, like in glassy media in the vicinity of the glass transition temperature. Physical ageing and rejuvenation have also already been reported for cement pastes [32,33]. In concentrated suspensions, the ageing kinetics (time evolution of the shear modulus for instance) is usually logarithmic, which is precisely the type of kinetics observed in this work (Fig. 12):

$$P_{ex} = C_1 \ln(1 + \Delta t) + C_2 \quad (5)$$

The C_1 parameter is strongly dependent on the viscosity of the interstitial fluid. At $w/c = 0.14$ in a PA based paste, C_1 increases from 0.33 to 1.27 when the p/c ratio decreases from 5 to 3%. At $w/c = 0.14$ and $p/c = 3\%$, exchanging PA for the more viscous HPMC decreases C_1 from 1.27 to 0.14. Thus, the higher the interstitial fluid viscosity, the lower the C_1 value is (the slower the ageing). This is qualitatively in agreement with a picture in which the collective rearrangements in a jammed system are controlled by the viscosity of the interstitial fluid in which the particles move.

Besides its fundamental interest, ageing is a factor which has to be carefully controlled for reproducible extrusion experiments. We observed that ageing is significantly slowed down if the pastes are compressed before extrusion. The compression step is thought to induce a shear of the paste which partially rejuvenates it. In addition, in order to minimize the variability of the results, we chose to consider, in the following, extrusion pressures interpolated at a constant ageing time of 20 min, referred to as $P_{ex}^{20\ min}$.

3.3.2. Extrusion pressure: w/c and p/c dependence

Fig. 13 displays the evolution of $P_{ex}^{20\ min}$ vs. *w/c* for PA containing pastes of varying *p/c* ratios. For a given *p/c* value, the higher *w/c*, the lower the extrusion pressure is. Qualitatively, this is a trivial result since water addition makes the paste more fluid. Quantitatively, the *w/c* dependence of the extrusion pressure at constant *p/c* may be fitted by a power law:

$$P_{ex}^{20min} = A^*(w/c)^{-\alpha} \quad (6)$$

The same type of dependence in *w/c* at constant *p/c* ratio is observed for HPMC or PEO containing pastes.

Fig. 14 shows the evolution of the extrusion pressure of PA containing pastes vs. *p/c* at constant *w/c* ratio. A decrease with increasing *p/c* is observed, according to a power law with exponent $\alpha = -2$:

$$P_{ex}^{20min} = a^*(p/c)^{\alpha} \quad (7)$$

Contrary to the *w/c* dependence of the extrusion pressure, this trend is far from being intuitively obvious. It cannot be explained in terms of interstitial fluid viscosity since the latter is increasing with *p/c*, whereas $P_{ex}^{20\ min}$ is decreasing. Possible interpretations will be scrutinized in the following section.

3.3.3. The pressure reduction mechanism

To consider *w/c* and *p/c* as independent parameters is not satisfying since changing *w/c* at constant *p/c* leads to a large change in solid volume fraction. In addition, it modifies the amount of entrained air. For those reasons, only the real cement volume fraction, ϕ_c^{Re}, will be used as parameter.

Fig. 15 displays $P_{ex}^{20\ min}$ vs. real cement volume fraction for PA containing pastes of varying *p/c* ratio. The following trends may be identified. At "low" real cement volume fraction, the extrusion pressure is but moderately dependent on polymer content. On the contrary, at "large" ϕ_c^{Re}, $P_{ex}^{20\ min}$ is very dependent on *p/c*; the *largest* extrusion pressures are obtained for the samples with the *lowest* polymer content, i.e. with the lowest interstitial fluid viscosity.

The comparison of the different polymers brings additional elements. As shown in Fig. 16, for a given *p/c* ratio (3%), the adsorbing polymer (PA) gives a higher extrusion pressure than the two non-adsorbing polymers, which are also those with the highest viscosity (HPMC and PEO).

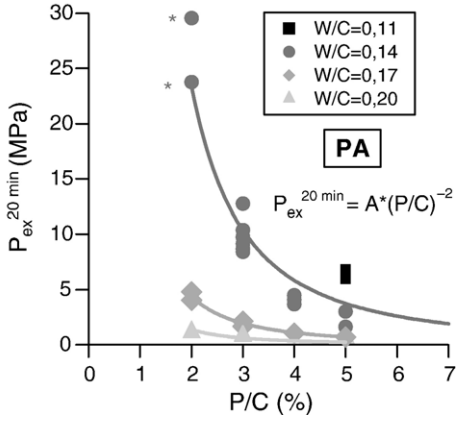

Fig. 14. Extrusion pressures interpolated at an ageing time of 20 min vs. *p/c* ratio for PA containing pastes. The stars indicate the extrusion pressures obtained with a barrel of 20 mm of diameter converted to values expected with a 30 mm diameter barrel, using Benbow's model.

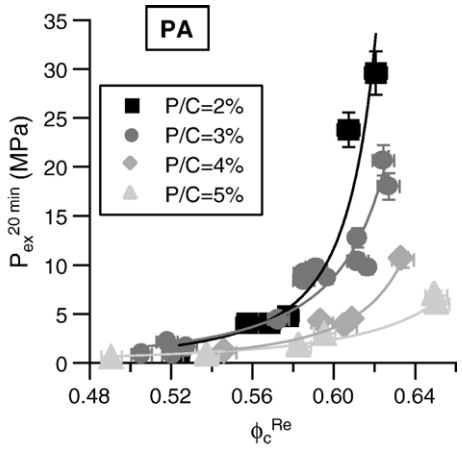

Fig. 15. Extrusion pressure interpolated at an ageing time of 20 min vs. effective cement volume fraction for PA containing pastes, at different *p*/*c* ratios.

A first point which should be considered for the interpretation of the previous data is precisely the adsorption and dispersion capacity of PA. A priori, the lowest extrusion pressures at the highest *p*/*c* ratios could be interpreted in terms of a larger adsorption and deflocculation efficiency. Indeed, the maximum packing fraction ϕ_m would be higher in a well dispersed state and, consequently, the ϕ/ϕ_m ratio and the extrusion pressure for a given ϕ would be lower, as observed (Fig. 15). However, this is not consistent with the fact that the polymer concentrations that we used are always well above those which are necessary to reach the plateau of the adsorption isotherm (Fig. 1). Therefore, no change in the dispersion state is expected when changing the polymer content. In addition, it is contradictory with the observation that the lowest extrusion pressures are obtained with the non-adsorbing polymers (Fig. 16).

Everything being considered, the results are better interpreted in terms of lubrication of interparticle contacts than in terms of particle dispersion state. Indeed, as discussed above, the very large increase of extrusion pressure obtained with PA at high ϕ_c^{Re} (Fig. 15) is observed at constant surface coverage and, hence, at constant dispersion state (at rest). Yet, the extrusion pressure decreases when more polymer is added. This is consistent with the hypothesis that the extrusion pressure is used to overcome interparticle friction and that this friction is facilitated by the polymer. In agreement with this, the larger the polymer concentration, the higher the cement volume fraction at which the extrusion pressure starts to diverge (Fig. 15).

Referring to Benbow's equation (Eq. (1)), the reduction of extrusion pressure due to the facilitated interparticle friction may stem from a decrease of the σ_y term and/or from a decrease of the τ_p term (the velocity-dependent terms do not vary since the experiments were performed at constant extrudate velocity). Thanks to the well-documented decrease in particle concentration at the walls which reduces the wall shear stress, it is likely that the main effect of the polymer is in the interparticle contact spots in the bulk [12].

Since all this happens at constant surface coverage in polymer (for PA), one is led to the conclusion that the lubrication involved is probably not "dry" lubrication but hydrodynamic lubrication. Once more, this is confirmed by the lower extrusion pressure obtained with the most viscous non-adsorbing polymer solutions (Fig. 16). Indeed, the efficiency of hydrodynamic lubrication is directly related to the viscosity of the fluid layer which has to be expelled when the particle surfaces approach each other. The conclusion of this discussion is that the critical factors for the paste extrusion pressure are the number of "direct" (unlubricated) interparticle contacts and the quality of lubrication in the lubricated contacts.

3.3.4. A free volume model of paste flow

There is increasing evidence that very concentrated suspensions belong to a class of dense systems generally known as "soft glassy systems" or "jammed" systems, in which viscosity depends – like in real glasses at temperatures slightly above the glass transition – on the so-called free volume v_f [34,35]. The free volume, which is a dynamic (depending on flow conditions) quantity, is defined as the excess unoccupied volume, per particle, available for cooperative rearrangements. The excess is determined with respect to the unoccupied volume when the particles are in close packed configuration (at $\phi=\phi_m$). Thus, we define

$$v_f/v_o = (1/\phi_c^{Re} - 1/\phi_m) \tag{8}$$

where v_o is the occupied volume. The divergence of the viscosity when ϕ_c^{Re} equals ϕ_m is related to the vanishing v_f.

In the following we will assume that the divergence of the extrusion pressure as ϕ_c^{Re} increases towards ϕ_m may be described in the same terms as the divergence of the viscosity, i.e. as a result of the vanishing free volume. In agreement with this, we chose to fit our experimental data with the following expression:

$$P_{ex}^{20min} = A[(\phi_m - \phi_c^{Re})^{-2} - \phi_m^{-2}] \tag{9}$$

This expression is akin to those used to describe the concentration dependence of the viscosity in concentrated pastes

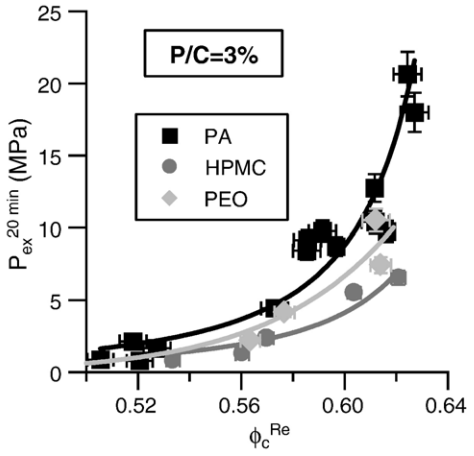

Fig. 16. Extrusion pressure interpolated at an ageing time of 20 min vs. effective cement volume fraction for pastes containing 3% w/w of various polymers.

Table 2
Parameters of the extrusion pressure model: $P_{ex}^{20\ min}=A.[(\phi_m-\phi_c^{eff})^{-2}-\phi_m^{-2}]$

	PA				HPMC	PEO
P/C (%)	2	3	4	5	3	3
ϕ_m (±0.005)	0.650	0.675	0.685	0.735	0.690	0.685
A (MPa)	0.030	0.050	0.025	0.045	0.034	0.043

[35,36]. It predicts, as it should, that the pressure diverges towards infinity when ϕ_c^{Re} reaches ϕ_m and, on the contrary, vanishes when $\phi_c^{Re}=0$. The parameter *A* is a reference pressure, considered as an adjustable parameter. The *A* and ϕ_m values thus obtained are listed in Table 2. Using a higher polymer content for PA containing pastes, or using a higher viscosity polymer for pastes of $p/c=3\%$ enables to increase ϕ_m and, hence, to extend the range of volume fractions in which the paste remains in a fluid-like state, which allows for denser packings to be processed.

With the ϕ_m values in hand, we calculated the free volume values, using Eq. (8). As a verification of the self-consistency of a free volume approach, we checked whether the extrusion pressure was indeed depending on the free volume, according to the classical relationships between free volume and viscosity. The reference behavior in glass forming liquids is the so-called Doolittle law [37]:

$$\eta = A.\exp\left[B.\frac{v_o}{v_f}\right] \tag{10}$$

Using $P_{ex}^{20\ min}$ instead of η, it was not possible to fit the data satisfyingly with this equation. However, the following law:

$$P_{ex}^{20min} = A.\exp\left[-B\frac{v_f}{v_o}\right] \tag{11}$$

or, equivalently

$$P_{ex}^{20min} = A.\exp\left[-B\left(\frac{1}{\phi_c^{Re}}-\frac{1}{\phi_m}\right)\right] \tag{12}$$

fits well the experimental data (see continuous lines in Figs. 15 and 16), with a single *B* value ($B=11$). This shows that the free volume is indeed the control parameter of the extrusion pressure, notwithstanding the fact that the observed relationship is not that which is usually observed in real glass-forming liquids. Whether there is or not polymer adsorbed on the cement particles does not matter, since the previous conclusion applies as well for PA and for HPMC and PEO.

The next question is to know what is or what are, in physical chemical terms, the parameter(s) which control(s) the free volume. Considering that the lubrication mechanism active in the pastes is hydrodynamic lubrication (see Section 3.3.3), it is reasonable to assume that the important parameter is the amount of polymer in the interstitial solution separating neighbouring particles. The product $e*\phi_p^{sol}$ of the average separation between particles, *e*, times the volume fraction of polymer in the interstitial solution, ϕ_p^{sol}, corresponds to this definition. The

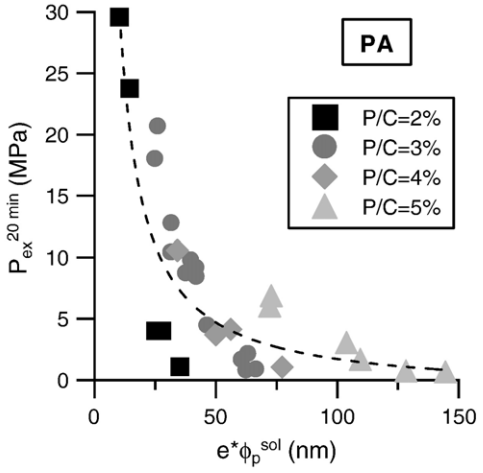

Fig. 17. Extrusion pressure vs. interfacial rate of active polymer for PA containing cement pastes prepared at different *p/c* ratios.

distance *e* may be calculated by dividing the volume of dispersing fluid in excess with respect to paste's saturation, by the Blaine surface area of the cement particles. It should be noted that *e* is a dynamic (flow conditions dependent) quantity. ϕ_p^{sol} is calculated by taking into account the amount of adsorbed polymer. Thus:

$$e*\phi_p^{sol} = \frac{2(1/\phi_c^{Re}-1/\phi_m)(p/c-p/c^{ads^o})}{\rho_p\Sigma_B(1/\phi_c^{Re}-1)} \tag{13}$$

where p/c^{ads} is the quantity of polymer required to form a monolayer of polymer adsorbed on particles, ρ_p the density of the polymer and Σ_B the Blaine surface area of the particles. $e*\phi_p^{sol}$, which may be called the interstitially active polymer rate, represents the volume fraction of confined polymer, per unit interface area, active in hydrodynamic lubrication.

As shown in Figs. 17 and 18, $e*\phi_p^{sol}$ seems indeed to rule the extrusion pressure, both for PA containing pastes and for the

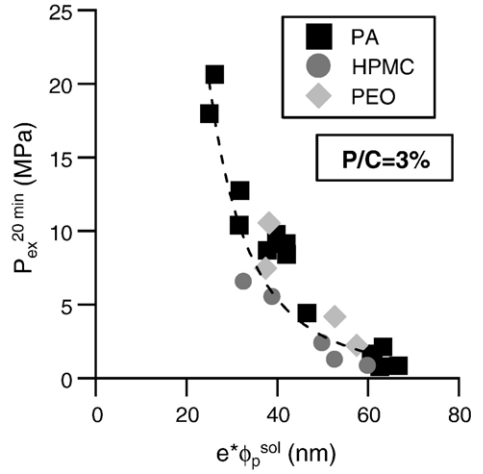

Fig. 18. Extrusion pressure vs. interfacial rate of active polymer for cement pastes prepared at a *p/c* ratio of 3%, for various polymers.

HPMC and PEO containing pastes. A reasonably good master curve is obtained in both cases. This confirms that polymer adsorption plays no role in the lubrication mechanism, which is hydrodynamic. It explains why the use of interstitial fluids with a higher viscosity leads to lower extrusion pressures, at constant cement volume fraction. The higher viscosity polymer solutions are better hydrodynamic lubricants since they are less easily expelled from the interparticle space.

The data points obtained with PA pastes at $p/c = 2\%$ (Fig. 17) are those which are the least well fitted by the master curve. It should be realized that the average interparticle separation in these conditions is only two or three times the polymer gyration radius. The later was calculated for a self-avoiding random coil conformation, by assuming that the mean squared end-to-end distance $<R^2>$ is ten times larger than that of an ideal Gaussian coil [38]. In spite of the electric charges on the polymer backbone, a random coil is a reasonable model, thanks to the large ionic strength screening the electrostatic repulsions (the electrostatic persistence length [39,40] is of the same order as a monomer unit length). The very concept of hydrodynamic lubrication in this confinement regime where interparticle separation reaches molecular dimensions is questionable.

4. Conclusion

In this work, we have shown that kneading of a cement paste is controlled by the viscosity and the volume of the dispersing fluid. During extrusion, both parameters (viscosity and volume) may be included in one single parameter: the interfacial (or interstitial) rate of active polymer. This parameter is *not* the amount of adsorbed polymer. It is the amount of polymer remaining in the solution in the gap between particles, per unit particle surface area. This implies that the mechanism of extrusion pressure reduction in extrusion is hydrodynamic lubrication of the contacts between particles in the converging extrusion flow.

References

[1] R. Srinivasan, D. Deford, S.P. Shah, The use of extrusion rheometry in the development of extruded fiber-reinforced cement composites, Concr. Sci. Eng. 1 (1999) 26–36.

[2] Y. Shao, J. Qiu, S.P. Shah, Microstructure of extruded cement-bonded fibreboard, Cem. Concr. Res. 31 (2001) 1153–1161.

[3] B. Mu, Z. Li, S.N.C. Chui, J. Peng, Cementitious composite manufactured by extrusion technique, Cem. Concr. Res. 29 (1999) 237–240.

[4] A. Peled, S.P. Shah, Processing effects in cementitious composites: Extrusion and Casting, ASCE J. of Mater in Civil Eng. 15 (2003) 192–199.

[5] K. Kendall, Interparticle friction in slurries, in: J. Briscoe, J. Adams (Eds.), Tribology in Particulate Technology, Adam Hilger, Bristol, 1987, pp. 91–102.

[6] H. Bohm, S. Blackburn, Effect of mixing procedure on fine alumina paste extrusion, Br. Ceram. Trans. 93 (1994) 169–177.

[7] M. Yang, H.M. Jennings, Influence of mixing methods on the microstructure and rheological behaviour of cement paste, Adv. Cem. Based Mater. 2 (1995) 70–78.

[8] A.J. McHugh, J.A. Walberer, Rheology and structuring in organo-ceramic composites, Compos., Part A Appl. Sci. Manuf. 32 (2001) 1085–1093.

[9] L.S. Tan, A.J. Mc Hugh, The role of particle size and polymer molecular weight in the formation and properties of an organo-ceramic composite, J. Mater. Sci. 31 (1996) 3701–3706.

[10] D. Chopin, F. de Larrard, B. Cazacliu, Why do HPC and SCC require a longer mixing time? Cem. Concr. Res. 34 (2004) 2237–2243.

[11] J. Benbow, J. Bridgewater, Paste Flow and Extrusion, 2nd ed., Oxford University Press, Oxford, 1993.

[12] H. Lombois-Burger, Malaxage et comportement rhéologique des pâtes granualires en présence de polymère : application à l'extrusion de formulations cimentaires, thesis, Université Pierre et Marie Curie (2003), 257 p.

[13] F. Merlin, H. Guitouni, H. Mouhoubi, S. Mariot, F. Vallée, H. Van Damme, Adsorption and heterocoagulation of nonionic surfactants and latex particles on cement hydrates, J. Colloid Interface Sci. 281 (2005) 1–10.

[14] T. Zhang, S. Shang, F. Yin, A. Aishah, A. Salmiah, T.L. Ooi, Adsorptive behaviour of surfactants on surface of Portland cement, Cem. Concr. Res. 31 (2001) 1009–1015.

[15] J. Rubio, J.A. Kitchener, The mechanism of adsorption of poly(ethylene oxide) flocculant on silica, J. Colloid Interface Sci. 57 (1976) 132–142.

[16] M. Lindheimer, E. Keh, S. Zaini, S. Partyka, J. Colloid Interface Sci. 138 (1990) 83–90.

[17] S. Mathur, B. Mohan Moudgil, Adsorption mechanism(s) of poly(ethylene oxide) on oxide surfaces, J. Colloid Interface Sci. 196 (1997) 92–98.

[18] P. Yu, R.J. Kirkpatrick, B. Poe, P.F. McMillan, J. Am. Ceram. Soc. 82 (1999) 742–748.

[19] C.B. Sawyer, J.S. Reed, Adsorption of hydroxypropyl methyl cellulose in an aqueous system containing multicomponent oxide particles, J. Am. Ceram. Soc. 84 (2001) 1241–1249.

[20] L. Nachbaur, P.C. Nkinamubanzi, A. Nonat, J.C. Mutin, Electrokinetic properties which control the coagulation of silicate cement suspensions during early age hydration, J. Colloid Interface Sci. (1998) 261–268.

[21] D. Bonen, S.L. Sarkar, The superplasticizer adsorption capacity of cement pastes, pore solution composition, and parameters affecting flow loss, Cem. Concr. Res. 25 (7) (1995) 1423–1434.

[22] S. Hanehara, K. Yamada, Interaction between cement and chemical Admixture from the point of cement hydration, absorption behaviour of admixture and paste rheology, Cem. Concr. Res. 29 (1999) 1159–1165.

[23] K. Yamada, S. Ogawa, S. Hanehara, Controlling the adsorption and dispersing force of polycarboxylate-type superplasticizer by sulfate ion concentration in aqueous phase, Cem. Concr. Res. 31 (2001) 375–383.

[24] K. Yamada, S. Hanehara, Interaction mechanism of cement and superplasticizers — the roles of polymer adsorption and ionic conditions of aqueous phase, Concr. Sci. Eng. 3 (2001) 135–145.

[25] Z. Tadmor, C.G. Gogos, Engineering Fundamentals — Characterization of Mixtures and Mixing, in: Principles of Polymer Processing, John Wiley & Sons, New York, 1979, pp. 196–242.

[26] N.A. Leighton, A. Acrivos, On the viscosity of a concentrated suspension of solid spheres, Rheol. Acta 27 (1967) 847–853.

[27] L.S. Tan, A.J. Mc Hugh, M.A. Gulgun, Evolution of mechano-chemistry and microstructure of a calcium aluminate-polymer composite: Part II. Mixing rate effects, J. Mater. Res. 11 (7) (1996) 1739–1747.

[28] J.A. Walberer, A.J. Mc Hugh, Processing/property/structure interactions in a calcium aluminate-phenol resin composite, Adv. Cem. Based Mater. 8 (1998) 91–100.

[29] S. Garrault-Gauffinet, A. Nonant, Experimental investigation of calcium silicate hydrate (C–S–H) nucleation, J. Cryst. Growth 200 (1999) 565–574.

[30] D. Bonn, P. Coussot, H.T. Huynh, F. Bertrand, G. Debregeas, Rheology of soft-glassy materials, Europhys. Lett. 59 (2002) 786–792.

[31] C. Derec, A. Ajdari, F. Lequeux, Rheology and ageing: a simple approach, Eur. Phys. J., E Soft Matter 4 (2001) 355–361.

[32] S.P. Jiang, J.C. Mutin, A. Nonat, Studies on the mechanism and physico-chemical parameters at the origin of cement setting. I. The fundamental processes involved during cement setting, Cem. Concr. Res. 25 (1995) 779–789.

[33] S.P. Jiang, J.C. Mutin, A. Nonat, Studies on the mechanism and physico-chemical parameters at the origin of cement setting. II. Physico-chemical parameters determining the coagulation process, Cem. Concr. Res. 26 (1996) 491–500.

[34] A.J. Liu, S.R. Nagel, Jamming is not just cool anymore, Nature 396 (1998) 21–22.

[35] V. Trappe, V. Prasad, L. Cipelletti, Jamming phase diagram for attractive particles, Nature 411 (2001) 772–775.

[36] D. Quemada, Rheology of concentrated dispersed systems and minimum energy dissipation principle. 1. Viscosity–concentration relationship, Rheol. Acta 16 (1977) 82–94.
[37] A.K. Doolittle, Newtonian flow. 1. The dependence of the viscosity of liquids on temperature, J. Appl. Phys. 22 (1951) 1031–1035.
[38] P.G. de Gennes, Scaling Concepts in Polymer Physics, Cornell University Press, 1979.
[39] T. Odijk, Polyelectrolytes near rod limit, J. Polym. Sci., B 15 (1977) 477–483.
[40] J. Skolnick, M. Fixman, Electrostatic persistence length of a wormlike polyelectrolyte, Macromol. 10 (1977) 944–948.